

## **BEHAVIOR AND DESIGN OF DIRECTLY LOADED LEDGES OF SHORT SPAN L-SHAPED BEAMS**

**Mohamed Nafadi, Omar Khalaf Alla, Gregory Lucier, Sami Rizkalla, Paul Zia, NC**  
State University, Raleigh, NC

and

**Gary Klein, Wiss, Janney, Elstner Associates, Northbrook, IL**

### **ABSTRACT**

*The current design procedure for ledges of L-shaped beams has been questioned by many engineers and researchers. Investigations by Klein (1986), Lucier et al. (2011) and others have indicated that the current ledge design equations may significantly overestimate the punching shear capacity of the ledge. This paper presents the findings of the first phase of a research project to investigate the effect of different parameters on the punching shear capacity of ledges of short span L-shaped beams. The investigation covers the parameters considered by the current PCI design procedure as well as additional parameters. Three-dimensional non-linear finite element analysis was used to complement the results of the experimental program. The paper also evaluates punching shear strength using an idealized failure surface that is consistent with the observed failure surfaces. Finally, recommendations are made on the nominal shear strength to be used for predicting the load carrying capacity of ledges for short span L-shaped beams.*

**Keywords:** L-shaped beams, Ledge, Punching shear, Spandrel

## INTRODUCTION

Precast concrete spandrel beams are typically used for parking structures and are considered one of the more complex products in the precast industry. The typical use of an L-shaped beam that supports precast double-tees for parking garages is shown in Figure 1(a). The ledge of an L-shaped beam typically runs the full length along the bottom of one face of the web to transfer the heavy eccentric loads, generated by the stems of the double-tee deck, to the beam. Therefore, the L-shaped beam is subjected to a series of eccentric concentrated loads, which cause vertical deflections as well as lateral displacements and rotations, as shown in Figure 1(b).

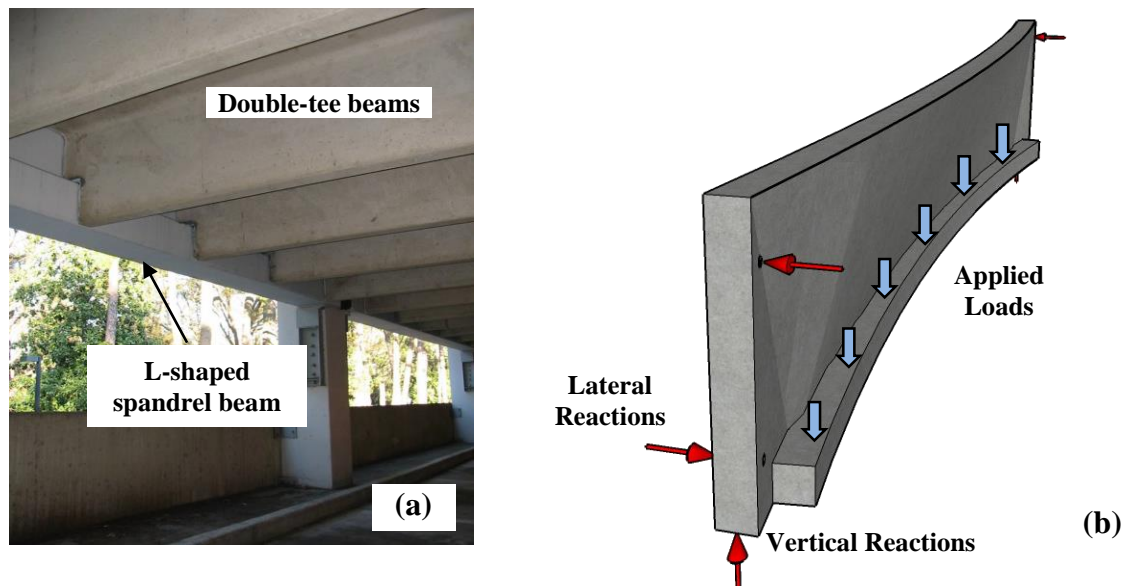


Figure 1: (a) Typical Spandrel Beam in a Parking Garage (b) Deformed Shape of L-shaped Beam

If the applied concentrated loads are sufficiently high, the ledge may fail in a localized punching shear mode. Such a failure mode is usually brittle in nature and accompanied by wide diagonal cracks that develop quickly. The exact shape of the failure surface depends on the location of the load within the span of the L-shaped beam. Two types of typical ledge failures can be identified by their location along the ledge: inner failures or end failures. The current PCI Design Handbook<sup>1</sup> assumes failure planes defined by 45-degree surfaces developing from the edges of the bearing pads. An idealized rectangular design surface is used to formulate equations for predicting the punching shear capacity of the ledge.

To date, there have been no reported ledge failures due to punching shear; however, findings from several laboratory tests and finite element modeling have indicated that the current ledge design equations may significantly overestimate the capacity of ledge. Thus, the safety margin provided by the current design procedure has been called into question, and there is a

need to develop an improved procedure for more accurate prediction of the ledge capacity of L-shaped beams.

Klein<sup>2-3</sup> conducted full-scale tests on three prestressed concrete spandrels; two L-shaped beams and one pocket spandrel. One of the two L-shaped beams failed due to punching shear in the ledge at a load level less than that estimated by the current PCI procedure. Klein pointed out that the PCI equations do not consider the effects of the global stress or the influence of eccentricity between the applied load and the centroid of the L-shaped cross section. Global stress and eccentricity were both assumed to reduce the ledge capacity.

Hassan<sup>4</sup> performed analytical modeling of Klein's specimens to investigate the influence of parameters believed to affect ledge behavior. The study referred to key parameters including the load eccentricity and the prestressing level, which can significantly affect the ledge capacity and are not taken into consideration by the current PCI procedure.

More recently, Lucier et al.<sup>5-7</sup> conducted an extensive experimental program on sixteen full-scale L-shaped beams, accompanied by finite element modeling to develop a rational design method for the L-shaped spandrel beams. Seven punching shear failures of the ledge were observed in five of the tested specimens. All measured failure loads were less than those predicted by current PCI procedures. The results also demonstrated that the punching shear capacity of the ledge is directly affected by the level of the global stresses in the beam.

Nafadi<sup>8</sup> conducted an extensive three-dimensional non-linear finite element analysis to evaluate the accuracy of the current PCI design procedure and to determine the relevant parameters believed to affect the ultimate strength of the ledge. The finite element model was first calibrated using the experimental results from Klein<sup>2-3</sup> and Lucier et al.<sup>5-7</sup>. A parametric study was performed to investigate the effect of 16 parameters for reinforced and prestressed concrete beams. The study concluded that the current PCI design procedure can overestimate the punching shear capacity of a ledge. Outputs of the analytical modeling were used to develop a comprehensive experimental program on short span and long span L-shaped beams to study selected key parameters believed to significantly affect the behavior.

This paper presents the findings of the first phase of a current experimental program undertaken to determine the effect of different parameters on the punching shear capacity of ledges in L-shaped beams. The short-span beams designed for the first phase experiments were intended to study the failure surface and parameters effecting punching shear strength without the influence of significant global stresses. The effect of global stresses will be studied in the second phase of the experimental program using long span beams.

## **EXPERIMENTAL PROGRAM**

The experimental program consisted of 17 short span L-shaped spandrel beams, including 6 duplicate beams, each 16'-6" long and simply supported with clear span of 15'-6". Each beam was tested at the mid-span and near the two ends for a total of three tests per beam. Thus the

total number of ledge tests was 51, including 17 mid-span tests and 34 tests near the ends of the ledge. The design of the test specimens was based on the nominal PCI design equations for the capacities of the ledge. All the specimens were produced at a precast plant on flat table forms, lying on their outer face. Steel cages and form dimensions were checked and samples of concrete and steel were taken to determine their material properties. A total of eleven parameters were considered in the experimental program. Five of these parameters are considered by the current design procedure of PCI including ledge height, ledge projection, bearing width, concrete strength, and edge distance of the load (for end failures). Six parameters that may affect the behavior of the ledges of L-shaped spandrel beams were included as determined by Nafadi<sup>8</sup>. These six parameters included load eccentricity from the inner web face, transverse steel (C bars), longitudinal steel in the ledge, bearing length, bearing type and effect of sustained load. A summary of the 17 short span beams is given in Table 1.

Table 1: Summary of Short Span L-shaped Test Beams

Beam	Design Concrete Strength	Ledge Height	Ledge Projection	Transverse Steel (C-bars)	Longitudinal steel in Ledge	Duplicate
RS1 (control beam)	7000 psi	8"	8"	#3@6"	2#4	x 2
RS2	5000 psi	8"	8"	#3@7"	2#4	x 1
RS3	10000 psi	8"	8"	#3@5"	2#4	x 2
RS4	7000 psi	12"	8"	#4@8"	2#5	x 1
RS5	7000 psi	10"	8"	#3@5"	2#5	x 2
RS6	7000 psi	10"	6"	#3@7"	2#4	x 1
RS7	7000 psi	10"	10"	#4@8"	2#5	x 2
RS8	7000 psi	8"	8"	#5@6"	2#4	x 1
RS9	7000 psi	8"	8"	#4@6"	2#4	x 2
RS10	7000 psi	8"	8"	#3@6"	3#6	x 1
RS11	7000 psi	8"	8"	#3@6"	2#6	x 2

The test beams were simply supported vertically using steel stands and were connected horizontally to columns of a testing frame at each end to maintain torsional equilibrium. The load was applied to the ledge by a steel beam which spanned between concrete blocks and the spandrel beam ledge. Hydraulic jacks were used to apply load to the steel beam, as shown in Figure 2 and Figure 3. The load was applied to the ledge through a special roller pin which allowed for rotation and horizontal displacement of the beam without changing the point at which the load was applied to the ledge. A rigid steel plate was used to distribute the applied load uniformly onto the ledge. The first test was conducted at mid-span to obtain an inner failure and then the loading system was moved to one end to achieve an end failure. Finally, the loading system was moved to the opposite end of the beam to achieve a second end failure. A load cell was used to measure the load applied by the hydraulic jack. String

potentiometers were used to measure the vertical and lateral displacements of the spandrel. Pi gages were used to measure concrete strains at different locations on the ledge and the web. All instruments were connected to an electronic data acquisition system to monitor the data during testing.

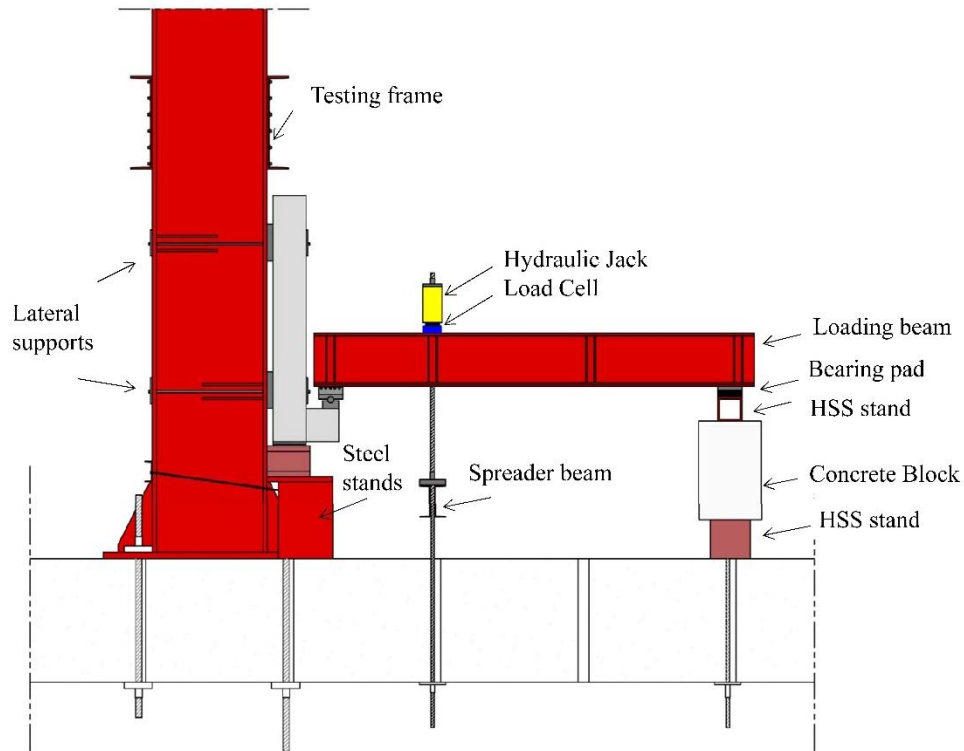


Figure 2: Schematic for Test Setup



Figure 3: Test at Mid-span (Inner Failure)

## TEST RESULTS

The concrete used for fabrication of the test beams was a normal weight structural concrete. Concrete sample cylinders were tested in compression at the time of ledge testing according to ASTM C39. Sections of the steel bars and wires were tested in tension to determine the mechanical properties of the steel for all reinforcing bar sizes and welded wire reinforcement used in the beams. The measured yield stresses for the different bar sizes and the welded wire reinforcement were 69 ksi and 92 ksi respectively. More details about the measured material properties are provided by Khalaf Alla<sup>9</sup>.

The observed failure mode for all 51 tests was punching shear in the ledge. Initially, a flexural crack at the ledge/web junction occurred. As the load was increased, the crack extended in length along the length of the ledge and propagated diagonally with an angle into the top face of the ledge. Prior to failure, additional cracks were observed to initiate at the back of the bearing plate and extended diagonally to the horizontal surface of the ledge. Failure occurred suddenly with diagonal tension cracks occurring on the front face of the ledge. The end failures exhibited similar behavior to the inner failures, however, the crack extended along the length of the spandrel until it reached the end of the ledge. The crack then extended on the side of the ledge until it reached the web. Figure 4(a), Figure 4(b) and Figure 4(c) show typical failure surfaces for both inner and end ledge failures respectively.



Figure 4: (a) Front View for Inner Ledge Failure (b) Front View for End Ledge Failure (c) Side View for End Ledge Failure

The measured ledge capacities are compared to the values predicted by the current PCI design procedure for both types of failures in Figure 5. For inner failures, the comparison indicates that the measured values range from 73 to 102 percent of the predicted values. For end failures, the measured values range from 79 to 158 percent of the prediction by the current PCI design procedure. Therefore, the test results confirm that the current PCI design procedure can overestimate the punching shear capacity of a ledge and such overestimation is more pronounced at inner locations than at end locations.

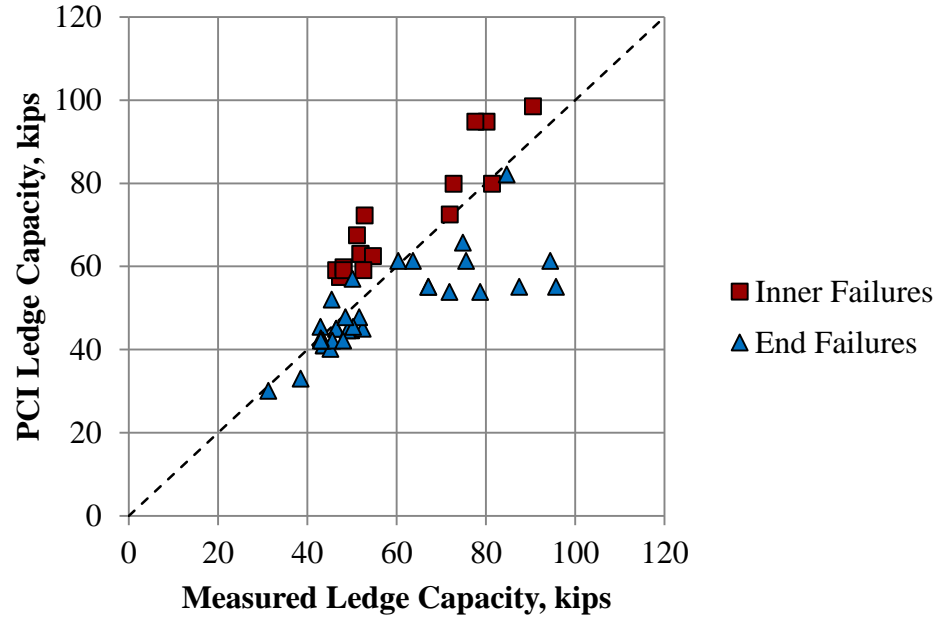


Figure 5: Comparison between the Measured and PCI Predicted Ledge Capacities

To highlight the effect of each parameter independently, the concrete compressive strength was normalized for all other parameters, where the measured punching shear load was normalized by the ratio  $\sqrt{\frac{f'_c}{f'_{cm}}}$  where,  $f'_c$  is the specified nominal compressive strength of concrete and  $f'_{cm}$  is the measured concrete compressive strength. The percent increase or decrease of the measured ledge capacity with respect to the increase of selected parameters considered in the study is shown in Figure 6.

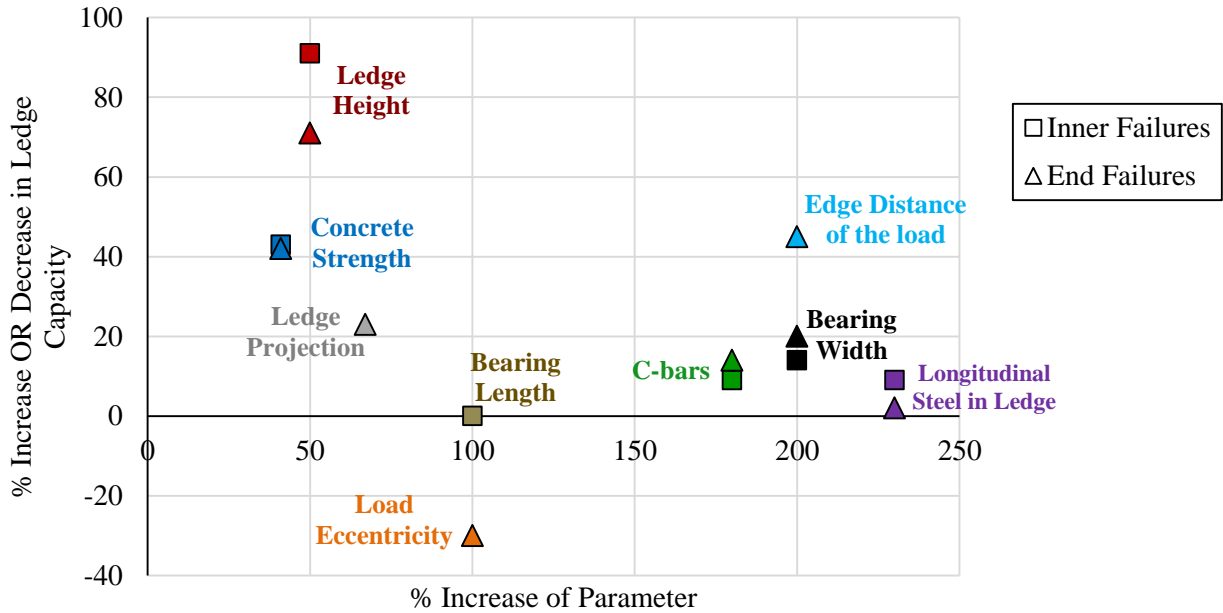


Figure 6: Effect of Selected Parameters

Figure 6 clearly indicates that four of the nine parameters have significant effect on the ledge capacity. They are ledge height, concrete compressive strength, load eccentricity and the edge distance of the applied load. The following sections provide brief discussions of these four parameters.

**1. Concrete Strength:** Test results at the inner locations indicated that increasing the concrete strength resulted in an increase of the ledge punching shear capacity in proportion to the square root of concrete strength. The measured result was also confirmed by the finite element analysis which covered a wider range of concrete strengths. The measured failure loads, the predicted values based on the current PCI design procedure, and the finite element predictions are shown in Figure 7(a). The FE analysis indicates that the ledge capacity increased by 40 percent when the square root of the concrete strength was increased by the same amount.

**2. Ledge Height:** The results clearly indicate that the ledge height is the most influential parameter on the punching shear capacity of the ledge. Test results indicate that the measured ledge capacity increased by 90 and 70 percent, for inner and end locations of the ledge, by increasing the ledge height from 8 to 12 inches, as shown in Figure 7(b).

**3. Load Eccentricity:** Test results indicate that increasing the load eccentricity, measured from the inner face of the web, decreases the ledge capacity, as shown in Figure 7(c). It should be noted that the current PCI design procedure does not account for this parameter, and therefore the ledge capacity is not be affected by the load eccentricity, as also shown in Figure 7(c).

**4. Edge Distance of the Load:** Test results indicate that increasing the edge distance of the applied load increases the ledge capacity, as shown in Figure 7(d). However, when the edge distance is increased more than twice the ledge height, the effect on the punching shear capacity of the ledge is negligible and the configuration of the failure surface is changed, as shown in Figure 8.

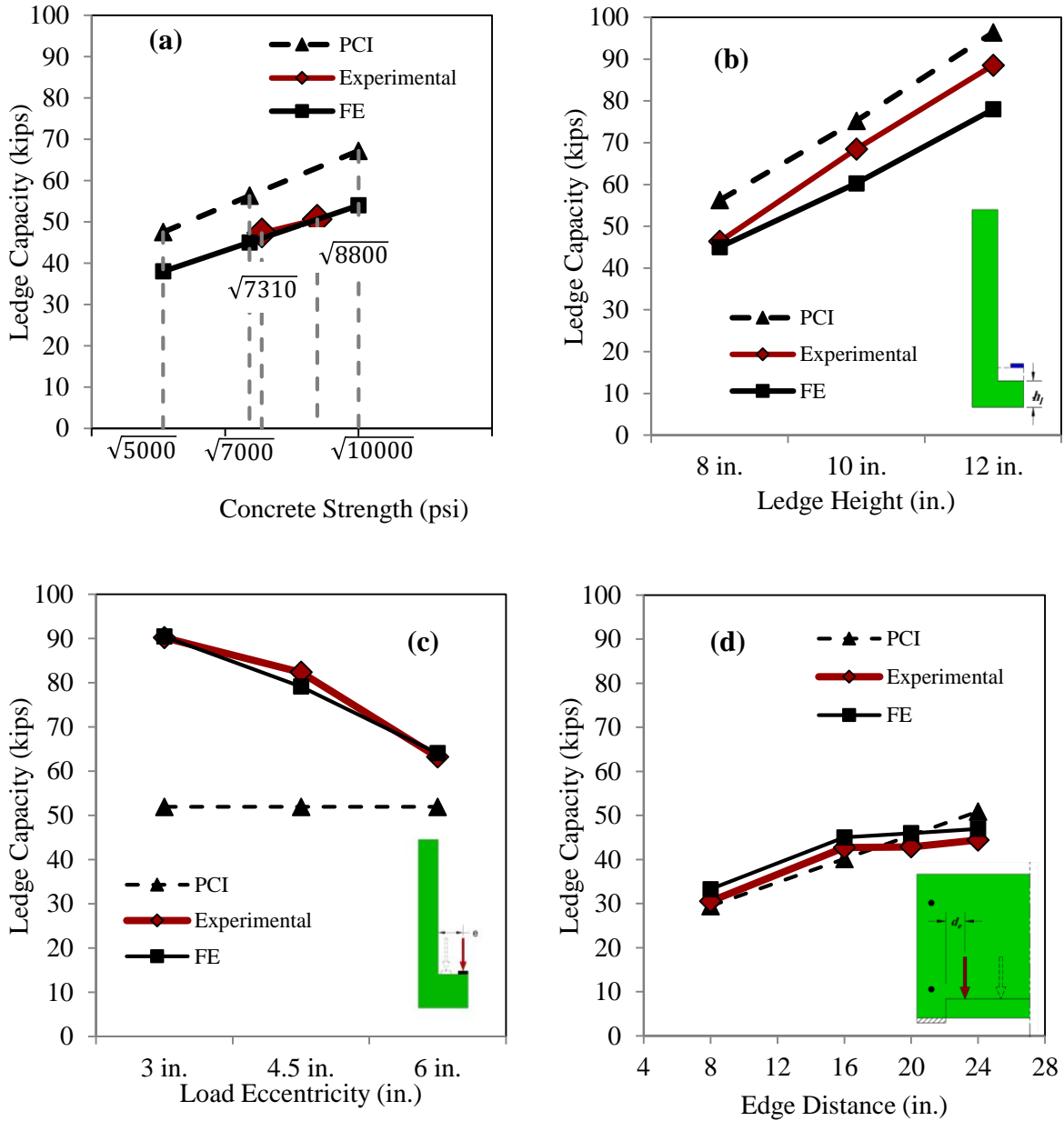


Figure 7: Effect of Selected Parameters (a) Concrete Strength (b) Ledge Height (c) Load Eccentricity from Inner Web Face (d) Edge Distance of the Load

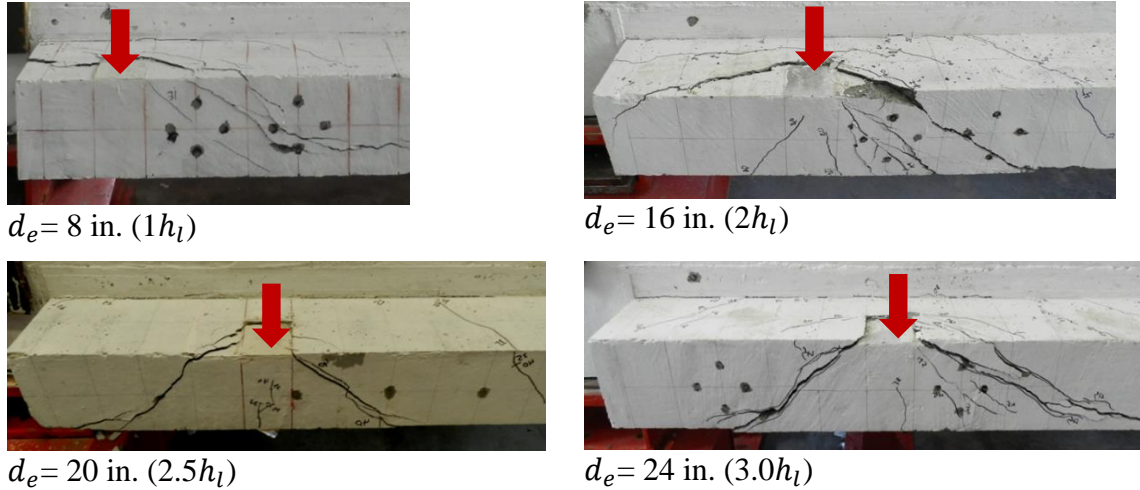


Figure 8: Effect of Edge Distance on Failure Surface

### CONFIGURATION OF THE FAILURE SURFACE

A typical failure surface is initiated by formation of cracks at the back of the bearing plate and extend horizontally on both sides at an angle of 27 degree, as shown in Figure 9(a). Then the cracks extend into the front face of the ledge with an angle that is dependent on the ledge height. For ledges of 8 in. height, the angle was 34 degrees, while for the ledges of 12 in. height, it was 45 degrees. If the edge distance of the applied load was less than twice the ledge height, the failure surface can be defined as an end failure, as shown in Figure 9(b). The cracked concrete was chipped off for several inner and end failures to measure the geometry of the failure surface. The bottom view of a typical failure surface, shown in Figure 9(c), indicates that the crack extended into the bottom of the beam and bypassed the hanger bars.

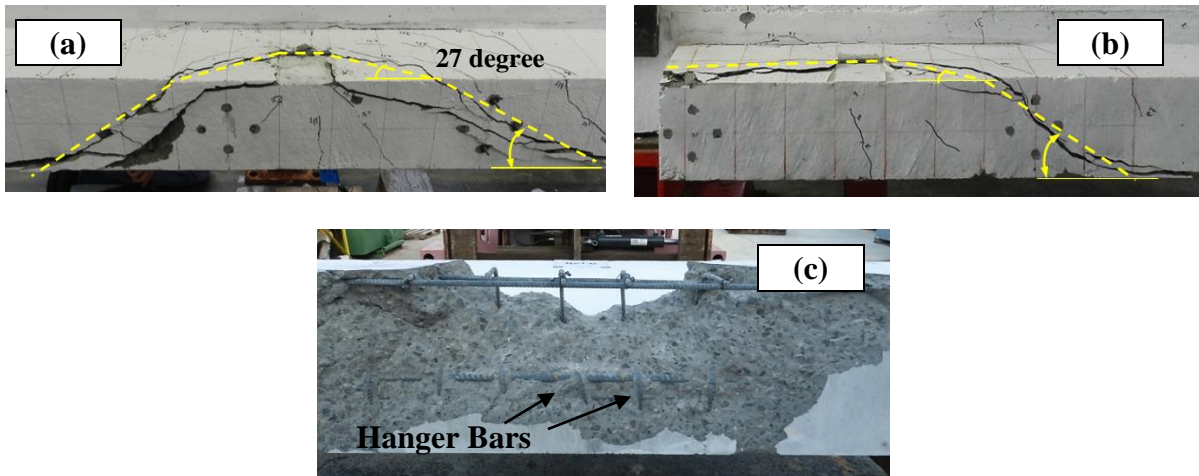


Figure 9: (a) Typical Inner Failure Surface (b) Typical End Failure Surface (c) Bottom View after Chipping Cracked Concrete

**EVALUATION OF PUNCHING SHEAR STRENGTH**

Based on the measured geometry of the failures, three idealized surfaces were considered for both inner and end failures. The corresponding shear strength for each idealized surface was determined based on the measured failure load, assuming uniform nominal shear stresses on the idealized failure planes. Statistical analysis was performed to determine the most appropriate idealization of the failure surface with respect to the geometry of the observed failure surfaces. The idealized failure surface is based on a horizontal angle of 27 degrees and a vertical angle of 34 degrees, as shown in Figure 10(a) for a typical inner failure. The same procedure was used to define the end failure surface, as shown in Figure 10(b).

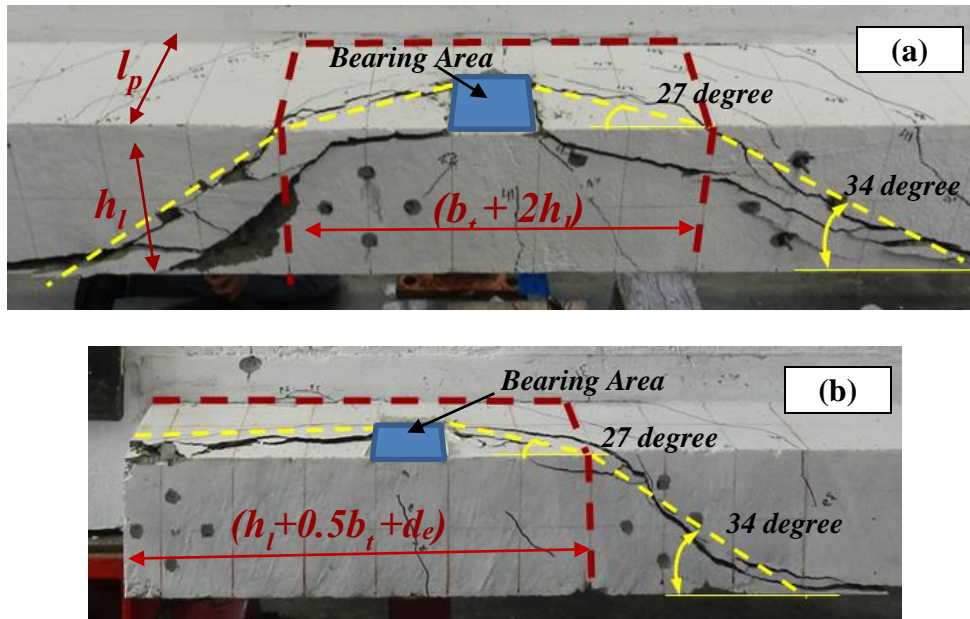


Figure 10: Idealized Failure Surfaces (a) Typical Inner Failure (b) Typical End Failure

The idealized failure surface area for the inner and end failures, and the corresponding recommended shear strength to predict the ledge capacity are given in Table 2.

Table 2: Calculated Shear Stresses for Inner Failures

	Idealized Failure Surface Area	Recommended Shear Strength
<b>Inner Failure</b>	$h_l(2h_l + b_t) + (2h_l l_p)$	$1.8 \sqrt{f'_c}$
<b>End Failure</b>	$h_l(h_l + 0.5b_t + d_e) + (h_l l_p)$	

Based on the research findings, two equations are proposed to predict the punching shear capacity of the ledge. The proposed equations are limited to short span reinforced concrete L-shaped spandrel beams where the global flexural and shear forces are less than 40 percent of the nominal flexural and shear capacities of the beam respectively. It should be noted that the

equations are limited to normal weight concrete. It is recommended to use the lesser value of the following two equations for the prediction of nominal punching shear capacity.

- $V_n = 1.8 h_l \sqrt{f'_c} (2h_l + b_t + 2 l_p)$
- $V_n = 1.8 h_l \sqrt{f'_c} (h_l + 0.5b_t + d_e + l_p)$

Where;

$V_n$ : Nominal shear strength, lb.

$h_l$ : Ledge height of the beam, in.

$b_t$ : Bearing width of the bearing plate, in.

$d_e$ : Edge distance from the center of applied load to the end of the beam, in.

$l_p$ : Ledge projection of the beam, in.

$f'_c$ : Specified concrete compressive strength, psi.

The predicted failure loads using the above equations are compared to the measured values as shown in Figure 11. The comparison clearly indicates the accuracy and safety of the recommended equations for predicting the ledge capacity of short span beams where the global flexural and shear loads are less than 40 percent of the nominal flexural and shear capacities of the beam respectively. When used for design, the nominal strength,  $V_n$ , should be multiplied by the strength reduction factor,  $\phi$ , for shear (0.75 in ACI 318-14).

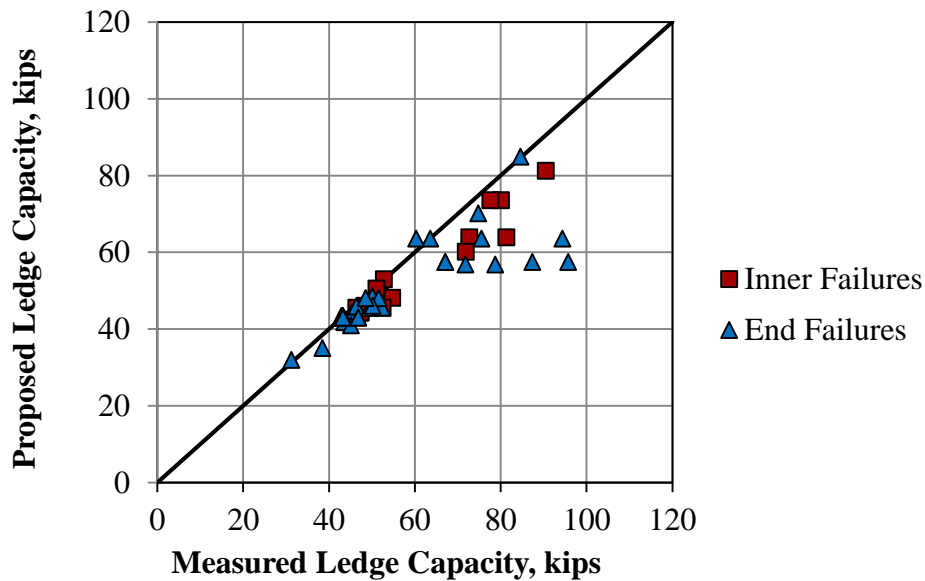


Figure 11: Proposed Ledge Capacities versus Measured Values

## CONCLUSIONS

Based on the findings of an extensive experimental program as well as FE analysis conducted to determine the punching shear capacity of ledges of L-shaped spandrel beams, the following conclusions can be drawn for the ledges of short span reinforced concrete L-shaped beams:

1. The current PCI design procedure overestimates the ledge punching shear capacity especially at the inner locations of the ledge.
2. The observed failure surface was different from the failure surface assumed by the current PCI design procedure. The failure initiated from the back of the bearing plate and extended with horizontal angles on the top surface of the ledge and extended on the front face of the ledge with angles shallower than that assumed by the current PCI design procedure.
3. A parametric study, including eleven parameters, indicated that the following four parameters have significant effect on the ledge punching shear capacity:
  - (a) Ledge height
  - (b) Concrete compressive strength
  - (c) Load eccentricity from inner web face
  - (d) Edge distance of the load
4. Based on the observed shape of the failure surface and the measured failure loads of the ledge at different locations, the following two equations are proposed for the nominal design shear strength of the ledge. The equations are limited to short span normal weight reinforced concrete beams and it is recommended that the lesser of the two should be used

- $V_n = 1.8 h_l \sqrt{f'_c} (2h_l + b_t + 2 l_p)$

- $V_n = 1.8 h_l \sqrt{f'_c} (h_l + 0.5b_t + d_e + l_p)$

## ACKNOWLEDGMENTS

This research was sponsored by the PCI Research and Development Committee. The authors are grateful to the ledge advisory committee for the support and guidance provided throughout the various phases of this research. The authors would also like to thank the PCI Producer Members who produced test specimens, and provided materials and expertise in support of the experimental program.

## REFERENCES

1. PCI Industry Handbook Committee, "PCI Design Handbook: Precast and Prestressed Concrete," 7th ed, Chicago, IL, 2010.

2. Klein, G.J., “Design of Spandrel Beams,” *PCI Journal*, V.31, No. 5, September-October 1986, pp. 76–124.
3. Klein, G. J., “Design of Spandrel Beams,” PCI Specially Funded R & D Program Research Project No. 5 (PCISFRAD #5), Prestressed Concrete Institute, Chicago, IL, 1986.
4. Hassan, T.K., “Finite Element Study of Shear Behavior of Spandrel Ledges and Comparison with PCI Shear Design Provisions,” *Advances in Structural Engineering*, V.10, No.5, October 2007, pp. 475–485.
5. Lucier, G., Walter, C., Rizkalla, S., Zia, P., and Klein, G., “Development of a Rational Design Methodology for Precast Concrete Slender Spandrel Beams: Part 1, Experimental Results,” *PCI Journal*, V.56, No. 2, April 2011, pp. 88–112.
6. Lucier, G., Walter, C., Rizkalla, S., Zia, P., and Klein, G., “Development of a Rational Design Methodology for Precast Concrete Slender Spandrel Beams: Part 2, Analysis and Design Guidelines,” *PCI Journal*, V.56, No. 4, October 2011, pp. 106–133.
7. Lucier, G., Walter, C., Rizkalla, S., Zia, P., and Klein, G., “Development of a Rational Design Methodology for Precast Concrete Slender Spandrel Beams,” Technical Report No. IS-09-10, 2010, Constructed Facilities Laboratory, North Carolina State University, Raleigh, NC.
8. Nafadi, M.K., “Analytical Modeling and Behavior of Ledges of L-shaped Beams,” MS Thesis, 2013, North Carolina State University, Raleigh, NC.
9. Khalaf Alla, O.M., “Design and Behavior of Ledges for Short Span L-Shaped Spandrel Beams,” MS Thesis, 2015, North Carolina State University, Raleigh, NC.